The forsterite–tephroite series: I. Crystal structure refinements

CARL A. FRANCIS

Mineralogical Museum, Harvard University
Cambridge, Massachusetts 02138

AND PAUL H. RIBBE

Department of Geological Sciences
Virginia Polytechnic Institute and State University
Blacksburg, Virginia 24061

Abstract

The crystal structures of the following metamorphic olivines, $M_2^{2+}[SiO_4]$, in the forsterite-tephroite (Fo–Te) series were refined in space group *Pbnm*:

	Cation composition M				Cell parameters (Å)			
	Mg	Mn	Ca	Fe	*a*	*b*	*c*	*R factor*
Fo_{51}	1.028	0.964	0.006	0.002	4.794	10.491	6.123	0.029
Te_{91}	0.181	1.780	0.013	0.026	4.879	10.589	6.234	0.039

Treating minor Fe and Ca as though they were Mn, the refined cation distributions (*esd*'s < 0.01) and mean bond lengths are:

	M(1) site				M(2) site			
	Mg	Mn	⟨M(1)–O⟩		Mg	Mn	⟨M(2)–O⟩	⟨Si–O⟩
Fo_{51}	0.92	0.08	2.116Å		0.11	0.89	2.185Å	1.637Å
Te_{91}	0.17	0.83	2.029Å		0.00	1.00	2.227Å	1.640Å

By comparison, a previously refined synthetic $Fo_{53}Te_{47}$ specimen "heat-treated at 1000°C" is significantly more disordered ($K_D = 0.196$) than the naturally occurring Fo_{51} ($K_D = 0.011$). As expected, mean M(1)–O and M(2)–O distances correlate linearly with Mg/(Mg+Mn) occupancy.

Introduction

With the widespread availability of automated X-ray diffractometers and least-squares refinement programs, order–disorder has become a principal theme of contemporary crystal chemical investigations (Burnham, 1973). Both natural and synthetic compounds with the olivine structure have been intensively studied (for a review, see Ganguli, 1977). At least 25 different room-temperature refinements of the geologically-important Mg–Fe olivines have been carried out and 13 additional refinements extend the observational conditions to temperatures of ~1000°C and pressures of ~50 kbar (Basso *et al.,* 1979; Birle *et al.,* 1968; Brown and Prewitt, 1973; Finger, 1970; Finger and Virgo, 1971; Hazen, 1976; Smyth, 1975; Smyth and Hazen, 1973; Wenk and Raymond, 1973).

However, the crystal structures of only two Mg–Mn olivines have previously been refined. One of them contains 11 mole percent of Zn_2SiO_4, thereby complicating the octahedral site refinement (Brown, 1970). The other is synthetic $Fo_{53}Te_{47}$ which was "heat treated at 1000°C" (Ghose and Weidner, 1974; Ghose *et al.,* 1976) and thus does not represent a naturally equilibrated Mg/Mn distribution. The present refinements were undertaken to examine Mg/Mn ordering in natural olivines uncomplicated by additional substituents.

Experimental procedures and structure refinement

The crystals used for refinement were selected from the suite of specimens described in Part II of this study (in preparation). The manganoan forsterite

from Långban, Sweden (Harvard University #116463) has the composition $Mg_{1.028}Mn_{0.964}Ca_{0.006}Fe_{0.006}SiO_4$. It occurs with fine-grained hausmannite in a calcite skarn. In hausmannite-free bands anhedral forsterite crystals range from 0.1–1.0 cm in size. The tephroite, from an unspecified location in Madagascar (Harvard University #108206) has the composition $Mn_{1.780}Mg_{0.181}Fe_{0.026}Ca_{0.013}SiO_4$. It occurs as discrete rounded crystals 1–2 mm in diameter associated with rhodonite, yellow spinel, and blue apatite in a calcite marble. For the purposes of site occupancy refinement these compositions were approximated as $Fo_{51}Te_{49}$ and $Te_{91}Fo_9$ and are denoted below as Fo_{51} and Te_{91}.

Refinements were carried out in the conventional but nonstandard space group *Pbnm*. Unit-cell dimensions (Table 1) were calculated from the orientation matrices and are identical to within three estimated standard deviations of those obtained by least-squares refinement of powder data as reported in Part II. The crystals used for data collection are tabular with dimensions 0.24 × 0.24 × 0.07 mm for Fo_{51} and 0.30 × 0.30 × 0.20 mm for Te_{91}. Intensity data were collected in two octants ($2\theta \leq 70°$) at 18°C on a Picker FACS-1 four-circle diffractometer, using Nb-filtered $MoK\alpha$ radiation ($\lambda = 0.70926$Å) and the ω–2θ scanning technique at a rate of 1° 2θ per minute. Twenty-second background measurements were made at either end of dispersion-corrected scan ranges. Two standard diffractions were monitored during data collection and used to calibrate the intensities by interpolation. The data were corrected for background, Lorentz, and polarization effects. Crystal shapes were approximated by polyhedral envelopes in the absorption correction. Linear absorption coefficients (μ) for $MoK\alpha$ are 47.7 cm^{-1} for Fo_{51} and 77.2 cm^{-1} for Te_{91}. Finally, the data were averaged to yield sets of 731 and 773 unique structure factors for Fo_{51} and Te_{91} respectively.

Full-matrix least-squares refinements of Fo_{51} and

Te_{91} were carried out using the program RFINE 4 (Finger and Prince, 1975). Scattering factors for neutral atoms with corrections for anomalous dispersion were taken from the *International Tables for Crystallography* (1974, p. 99, 149). The refinements were initiated using the positional parameters of forsterite (Hazen, 1976), fully ordered cation distributions [Mg concentrated on M(1)], and reasonable isotropic temperature factors. After several cycles varying the scale factor and positional parameters, the conventional R factor dropped to ~0.10. Site occupancy refinements were undertaken by varying the Mg content of M(1) while constraining the total cation chemistries to agree with the observed compositions. Site occupancies were refined alternately with isotropic temperature factors, and the R factors decreased to $R = 0.038$ for Fo_{51} and $R = 0.056$ for Te_{91}; all positional parameters were identical within three estimated standard deviations to those of the final anisotropic model. Anisotropic thermal parameters and an isotropic extinction correction were applied in the final cycles of both refinements, leading to unweighted R factors for all data of 0.029 for Fo_{51} and 0.038 for Te_{91}.

Structure factors for which $F_{obs} < 2\sigma F_{obs}$ were considered unobserved and were excluded from the refinement. These are indicated in the structure factor tables (Tables 2a,b)[1] by asterisks. Atomic coordinates are listed in Table 3, anisotropic temperature factors, equivalent isotropic temperature factors, and their root-mean-square equivalents are listed in Table 4, and interatomic distances and interbond angles are recorded in Table 5.

The olivine structure

The olivine structure is so well-known that only a brief description is given here. [For structure diagrams the reader is referred to Birle *et al.* (1968) and Hazen (1976).] It consists of a slightly distorted hexagonal closest-packed array of oxygen anions with one-half of the octahedral sites filled with divalent cations and one-eighth of the tetrahedral sites occupied by silicon. The key structural feature is the serrated chain, parallel to *c*, of two symmetrically-independent, edge-sharing octahedra. The M(1) octahedron is at the interior of the chain and the M(2) octahedron forms the "elbows" of the chain.

Table 1. Crystal data

	Fo_{51} Langban, Sweden	Te_{91} Madagascar
a	4.794(2)*A	4.879(2) A
b	10.491(4)	10.589(4)
c	6.123(2)	6.234(3)
Vol	308.7(2) A^3	322.1(2) A^3
Density (calc.)	3.67 g/cc	4.06 g/cc

*Numbers in parentheses represent estimated standard deviation (1$\hat{\sigma}$) and refer to the last decimal place.

[1] To obtain a copy of Table 2, order Document AM-80-141 from the Business Office, Mineralogical Society of America, 2000 Florida Avenue, NW, Washington, DC 20009. Please remit $1.00 in advance for the microfiche.

Table 3. Atomic coordinates

Atom	Fo$_{51}$ x	y	z
M(1)			
M(2)	0.9870(1)	0.2790(1)	¼
Si	0.4226(2)	0.0910(1)	¼
O(1)	0.7585(5)	0.0867(2)	¼
O(2)	0.2301(5)	0.4489(2)	¼
O(3)	0.2782(3)	0.1590(2)	0.0374(2)

Atom	Te$_{91}$ x	y	z
M(1)			
M(2)	0.9877(2)	0.2801(1)	¼
Si	0.4265(4)	0.0951(2)	¼
O(1)	0.7574(10)	0.0914(5)	¼
O(2)	0.2162(11)	0.4525(5)	¼
O(3)	0.2857(8)	0.1625(3)	0.0401(5)

The [SiO$_4$] tetrahedron shares its basal edges with two M(1) and one M(2) octahedra. Its apex links to the adjacent chain, which is related to the first by *b*-glide planes.

Cation ordering

Consideration of cation ordering in non-calcium olivines began with the prediction of Ghose (1962) that because the effective ionic radius of Fe (r = 0.78Å) is larger than that of Mg (r = 0.72Å) it should be preferentially ordered into the larger M(2) site. Refinements of four compositions across the forsterite–fayalite series by Birle *et al.* (1968) and refine-

ments by Brown (1970) failed to detect Mg/Fe order. Subsequent refinements by Finger (1970), Finger and Virgo (1971), Brown and Prewitt (1972), Wenk and Raymond (1973), Ghose *et al.* (1976), and Basse *et al.* (1979) have shown small but significant degrees of ordering of Fe onto M(1) rather than M(2). This unexpected result, termed anti-ordering by Brown and Prewitt (1973), has generally been attributed to the greater distortion from ideal O$_h$ symmetry of the [M(1)O$_6$] octahedron which results in a slightly greater crystal field stabilization energy for Fe^{2+} on M(1) (Walsh *et al.*, 1974) [although for some Mg-rich olivines, Fe^{2+} may show a slight preference for M(2) (Wenk and Raymond, 1973)]. In general, site preference of divalent transition-metal cations relative to Mg in olivine is determined by two competing factors: cation size and crystal field effects (Rajamani *et al.*, 1975).

Divalent manganese has a high spin d^5 configuration which is unaffected by crystal field effects. Thus cation ordering in Mg–Mn olivines is predicted (Brown, 1970; Burns, 1970, p. 118) to be governed by the size criterion with Mg (r = 0.72Å) preferring M(1) and Mn (r = 0.83Å) preferring M(2). The cation distributions determined in the present refinements and an earlier refinement of a synthetic manganoan forsterite (Fo$_{53}$Te$_{47}$) "heat treated at 1000°C" by Ghose and Weidner (1974) confirm the predicted preferences (Table 6). Another refinement, that of Mn$_{1.300}$Mg$_{0.345}$Zn$_{0.227}$Fe$_{0.128}$SiO$_4$ from Franklin, New Jersey (Brown, 1970) is consistent with but is not a

Table 4. Anisotropic temperature factors (β_{ij}), equivalent isotropic temperature factors (Beq) and their root-mean-square equivalents (μ)

	Atom	β_{11}*	β_{22}	β_{33}	β_{12}	β_{13}	β_{23}	B_{eq} (A^2)	μ(A)
Fo$_{51}$									
	M(1)	3.1(4)	1.35(8)	2.5(2)	−0.1(2)	−0.5(2)	−0.34(9)	0.42	0.073
	M(2)	6.1(2)	1.16(4)	3.66(9)	0.24(8)	0.0	0.0	0.54	0.083
	Si	3.1(3)	0.96(6)	2.5(2)	0.0(1)	0.0	0.0	0.36	0.068
	O(1)	2.2(7)	1.7(2)	3.7(4)	−0.2(3)	0.0	0.0	0.50	0.079
	O(2)	4.0(8)	1.1(2)	3.8(4)	−0.5(3)	0.0	0.0	0.48	0.078
	O(3)	3.9(6)	1.3(1)	3.6(3)	0.0(2)	0.0(3)	0.4(2)	0.50	0.079
Te$_{91}$									
	M(1)	5.8(4)	2.2(1)	4.8(2)	0.0(2)	−0.7(3)	−0.7(1)	0.76	0.098
	M(2)	6.7(4)	1.37(7)	5.0(2)	0.1(2)	0.0	0.0	0.68	0.093
	Si	5.4(7)	1.4(1)	4.5(3)	0.1(3)	0.0	0.0	0.61	0.089
	O(1)	2.9(18)	2.5(4)	6.7(10)	0.1(8)	0.0	0.0	0.81	0.101
	O(2)	5.7(18)	1.4(4)	5.6(9)	−0.2(7)	0.0	0.0	0.69	0.094
	O(3)	7.5(13)	1.9(3)	4.9(6)	0.2(5)	0.0(8)	0.4(3)	0.77	0.099

*β_{ij} is in the expression exp−($\beta_{11}h^2+\beta_{22}\kappa^2+\beta_{33}\ell^2+\beta_{12}2h\kappa+\beta_{13}2h\ell+\beta_{23}2\kappa\ell$) and values are quoted ×10^3.

Table 5A. Interatomic distances (Å) and angles (°) of Fo$_{51}$

[SiO$_4$] tetrahedron

Si–O(1)[1]	1.611(3)*	
O(2)[1]	1.661(2)	
O(3)[2]	1.638(2)	
Mean	1.637	

O...O distances		Angles at Si
O(1)-O(2)[1]	2.753(3)	114.6(1)
O(1)-O(3)[2]	2.752(3)	115.8(1)
O(2)-O(3)[2]a	2.560(3)	101.8(1)
O(3)-O(3)[1]a	2.604(3)	105.3(1)
Mean	2.664	109.2

[M(1)O$_6$] octahedron

M(1)-O(1)[2]	2.124(2)	
O(2)[2]	2.075(2)	
O(3)[2]	2.148(2)	
Mean	2.116	

O...O distances		Angles at M(1)
O(1)-O(2)[2]b	2.753(3)	85.35(7)
O(1)-O(2)[2]	3.087(1)	94.65(7)
O(1)-O(3)[2]	2.752(3)	85.93(8)
O(1)-O(3)[2]	3.126(3)	94.07(8)
O(2)-O(3)[2]	2.560(3)	105.38(8)
O(2)-O(3) 2	3.359(3)	74.62(8)
Mean	2.940	90.0

[M(2)O$_6$ octahedron]

M(2)-O(1)[1]	2.296(2)	
O(2)[1]	2.129(2)	
O(3)[2]	2.287(2)	
O(3)[2]	2.126(2)	
Mean	2.209	

O...O distances		Angles at M(2)
O(1)-O(3)[2]b	2.752(3)	78.90(7)
O(1)-O(3)[2]	3.197(3)	92.53(7)
O(2)-O(3)[2]	3.316(3)	97.28(8)
O(2)-O(3)[2]a	3.359(3)	90.09(7)
O(3)-O(3)[1]a	2.604(3)	69.40(8)
O(3)-O(3)[2]	3.010(3)	89.12(6)
O(3)-O(3)[1]	3.520(3)	111.70(9)
Mean	3.116	Mean 89.75

Table 5B. Interatomic distances (Å) and angles (°) of Te$_{91}$

[SiO$_4$] tetrahedron

Si–O(1)[1]	1.613(5)*	
O(2)[1]	1.663(6)	
O(3)[2]	1.641(4)	
Mean	1.640	

O...O distances		Angles at Si
O(1)-O(2)[1]	2.737(7)	113.3(3)
O(1)-O(3)[2]	2.750(6)	115.4(2)
O(2)-O(3)[2]a	2.580(6)	102.7(2)
O(3)-O(3)[1]a	2.617(6)	105.8(3)
Mean	2.669	109.2

[M(1)O$_6$]octahedron

M(1)-O(1)[2]	2.183(4)	
O(2)[2]	2.144(4)	
O(3)[2]	2.228(4)	
Mean	2.185	

O...O distances		Angles at M(1)
O(1)-O(2)[2]b	2.737(7)	86.26(15)
O(1)-O(2)[2]b	3.158(2)	93.74(15)
O(1)-O(3)[2]b	2.750(6)	85.20(16)
O(1)-O(3)[2]b	3.247(5)	94.80(16)
O(2)-O(3)[2]	2.580(6)	107.69(16)
O(2)-O(3)[2]	3.530(6)	72.31(16)
Mean	3.000	Mean 90.0

[M(2)O$_6$] octahedron

M(2)-O(1)[1]	2.292(5)	
O(2)[1]	2.139(5)	
O(3)[2]	2.318(4)	
O(3)[2]	2.147(3)	
Mean	2.227	

O...O distances		Angles at M(2)
O(1)-O(3)[2]b	2.750(6)	80.72(14)
O(1)-O(3)[2]	3.175(5)	91.26(12)
O(2)-O(3)[2]	3.355(b)	97.59(15)
O(2)-O(3)[2]a	3.350(6)	89.84(12)
O(3)-O(3)[1]a	2.617(6)	68.73(17)
O(3)-O(3)[2]	3.102(4)	87.94(8)
O(3)-O(3)[1]	3.617(6)	114.77(20)
Mean	3.172	Mean 89.85

*Number in parentheses represents one estimated standard deviation ($\hat{\sigma}$) and refers to the last decimal place.

a. Edges shared between tetrahedron and octahedron.

b. Edge shared between octahedra.

*Number in parentheses represents one estimated standard deviation ($\hat{\sigma}$) and refers to last decimal place.

a. Edge shared between tetrahedron and octahedron.

b. Edge shared between octahedra.

valid test of the prediction, because Mg had to be assigned to M(1) in order to simplify the computation.

The degree of order for the three pure Mg–Mn olivines is illustrated in Figure 1, with data for Mg–Fe olivines included for comparison. Order is frequently quantified by the use of a distribution coefficient K_D = [Mg/(Mg+Mn)M(2)][Mn/(Mg+Mn)M(1)]/[Mg/(Mg+Mn)M(1)][Mn/(Mg+Mn)M(2)] written for the ion exchange reaction Mg^{2+}M(1) + Mn^{2+}M(2)$\leftrightarrows$Mg^{2+}M(2) + Mn^{2+}M(1). For a fully ordered distribution K_D = 0, for a completely random distribution K_D = 1, and for an anti-ordered distribution K_D = ∞. These define the top and right edges, the long diagonal, and the left and bottom edges of the parallelogram in Figure 1.

The Mg–Mn olivines are strongly ordered by comparison with Mg–Fe olivines. The contrast between the heat-treated synthetic crystal (K_D = 0.196) and the metamorphic crystals (K_D = 0.000, 0.011) demonstrates that the degree of Mg/Mn order is dependent

Table 6. Refined site occupancies of Mg–Mn olivines

	M(1)				
Composition	Mg	Mn	Mg	Mn	K_D**
$Fo_{53}Te_{47}$*	0.724	0.276(4)	0.339	0.661	0.196
$Fo_{51}Te_{49}$	0.921(5)	0.079	0.110	0.890	0.011
$Fo_{09}Te_{91}$	0.172(9)	0.828		1.000	0.000

*Ghose & Weidner (1974).

**$K_D = \dfrac{[Mg/(Mg+Mn)M(2)][Mn/(Mg+Mn)M(1)]}{[Mg/(Mg+Mn)M(1)][Mn/(Mg+Mn)M(2)]}$

† Estimated standard deviations are in square brackets and refer to the last decimal place.

on a specimen's thermal history. However, the rarity of Mg–Mn olivines seems to preclude their wide use as petrogenetic indicators.

Stereochemistry

The steric details of non-calcium olivine structures, which arise from cation–cation repulsions across shared polyhedral edges, have been thoroughly discussed by Birle *et al.* (1968) and Brown (1970). One surprising result of the latter study is the constancy of Si–O distances irrespective of octahedral cation chemistry. The Si–O distances observed in this study (Table 5) are typical, being statistically indistinguishable from the corresponding values for ten olivines studied by Brown. In contrast, mean M–O distances are a linear function of the calculated effective

radii (Brown, 1970). This relationship is illustrated in Figure 2 for (Mg–Mn)-containing octahedra. The data (Table 7) fall into two distinct populations described by the following regression equations:

$$\langle M(1)-O \rangle = 2.200 - 0.096\,\%Mg; \quad R = 0.997$$

$$\langle M(2)-O \rangle = 2.223 - 0.097\,\%Mg; \quad R = 0.998$$

reflecting the inherent size difference between M(1) and M(2) octahedra due to the difference in number of shared edges.

Quadratic elongation, a measure of distortion often used in the analysis of finite homogenous strain, correlates linearly with bond angle variance for a large number of coordination polyhedra in minerals which show variations in both bond length and bond angle (Robinson *et al.*, 1971).

Using the bond angle variance parameter as a convenient measure of polyhedral distortion, Robinson *et al.* (1971) have shown that distortions of olivine [SiO₄] tetrahedra decrease with the weighted mean M–O distance, whereas distortions of olivine octa-
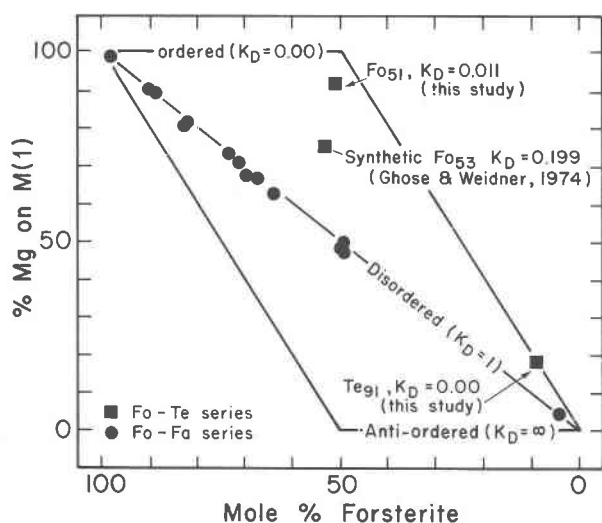

Fig. 1. Plot of percent magnesium on M(1) as a function of mole percent forsterite component, which illustrates the degree of cation order–disorder in the forsterite–tephroite series (squares) and the forsterite–fayalite series (dots). Data from Table 7.
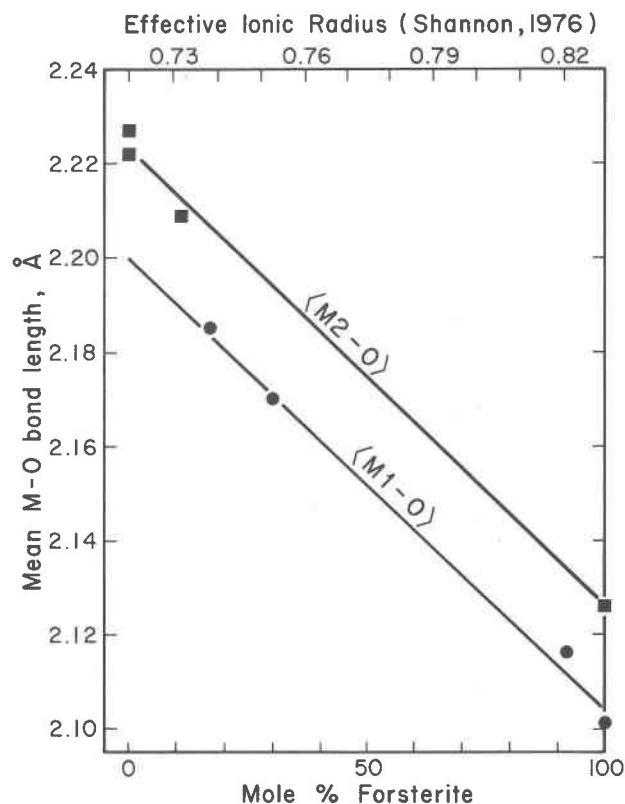

Fig. 2. Plot of mean M(1)–O (dots) and M(2)–O (squares) distances as a function of refined site occupancy in percent magnesium (lower abscissa) and effective ionic radius (upper abscissa). Lines represent regression equations given in the text.

Table 7. Mean M–O distances for (Mg,Mn)-containing octahedra

Mineral	Site	Occupancy	$<M-O>$(A)	Reference
Forsterite	M(1)	$Mg_{1.00}$	2.101	Hazen (1976)
	M(2)	$Mg_{1.00}$	2.126	
$Fo_{51}Te_{49}$	M(1)	$Mg_{0.92}Mn_{0.08}$	2.116	This study
	M(2)	$Mn_{0.89}Mg_{0.11}$	2.209	
$Te_{91}Fo_9$	M(1)	$Mn_{0.83}Mg_{0.17}$	2.185	This study
	M(2)	$Mn_{1.00}$	2.227	
Manganhumite	M(1)	$Mn_{0.70}Mg_{0.30}$	2.170	Francis & Ribbe (1978)
	$M(2)_6$	$Mn_{1.00}$	2.222	

Table 8. Polyhedral distortions as measured by the bond angle variance parameter $(\sigma)^2$ of Robinson et al. (1971)

Polyhedron	$Fo_{100}†$	Fo_{51}	Te_{91}
$[SiO_4]^*$	42.4	48.3	38.0
$[M(1)O_6]^{**}$	98.7	99.9	127.3
$[M(2)O_6]^{**}$	90.1	114.7	124.1

†Hazen (1976)

$^*\sigma(tet)^2 = \sum_{i=1}^{6} (\Theta_i - 109.47°)^2/5$

$^{**}\sigma(oct)^2 = \sum_{i=1}^{12} (\Theta_i - 90°)^2/11$

hedra increase with increasing M–O distance. Polyhedral distortions of the present structures (Table 8) conform to these general trends, but the distortions of Fo_{51} are somewhat anomalous. The M(2) octahedron is more distorted than M(1), reversing the general rule for end members and disordered compositions. The tetrahedron in Fo_{51} is also significantly more distorted than in either end member. These anomalies, which also hold for monticellite (Lager and Meagher, 1978), are attributed to the large size difference between M(1) and M(2) cations.

Reinterpretation of cation distribution in Zn,Mg tephroite

Brown (1970) reported the M(2) site occupancy of the Franklin, New Jersey tephroite to be

Table 9. Comparison of site occupancy models for $(Mn_{1.300}Mg_{0.345}Zn_{0.225}Fe_{0.128})SiO_4$

	Occupancy	Scattering Power* Electrons	Effective Ionic Radius (A)	$<M-O>$ obs. (A)	(A) pred.
Brown (1970)					
M(1)	$Mn_{0.432}Mg_{0.345}Zn_{0.180}Fe_{0.043}$	21.46	0.774	2.148	
M(2)	$Mn_{0.868}Fe_{0.085}Zn_{0.045}$	25.32	0.821	2.224	
Reinterpretation					
M(1)	$Mg_{0.345}Mn_{0.300}Zn_{0.227}Fe_{0.128}$	21.78	0.765		2.15†
M(2)	$Mn_{1.00}$	25.00	0.830		2.223††

$^*\sum n_i z_i$

$^{**}\sum n_i r_i$ (radii from Shannon (1976))

†Predicted from 0.765 + 1.38 (radius of ^{iv}O)

††Predicted from $<M(2)-O> = 2.223 - 0.097\%Mg$

$Mn_{0.868}Fe_{0.085}Zn_{0.045}$, with a mean M(2)–O distance of 2.224Å. Comparison of this mean bond length with the observed values of 2.229Å for $\langle M(2)-O \rangle$ in Te_{91} and 2.222Å for $\langle M(2)_6-O \rangle$ in manganhumite (Francis and Ribbe, 1978), both of which are completely occupied by Mn, suggests that the M(2) site in the Franklin tephroite is also completely occupied by Mn. The plausibility of a fully ordered distribution may be tested by comparing the effective X-ray scattering factors and ionic radii of the composite octahedrally coordinated atoms of the refined model with those of the fully ordered model. Only if these parameters are nearly equal can the ordered model be realistic. This comparison is made in Table 9. Scattering factors were approximated by summing the products of the atom fractions times their respective atomic numbers, which equal the number of electrons in neutral atoms. The scattering factors of both models are identical within the limits of resolution of X-rays for both M(1) and M(2). Similarly the mean effective radii of the divalent cations are nearly identical. Thus the intensity data are equally satisfied by the model reported by Brown (1970) and the fully ordered model. In further support of the ordered model may be cited the strong preference of Mg for M(1) observed in this study, the preference of Fe for M(1) discussed above, and the preference of Zn for M(1) relative to Mg (Ghose and Weidner, 1974). The ordered model therefore is not only possible but appears to be crystal-chemically preferable.

Acknowledgments

References

Basso, R., A. Dal Negro, A. Della Giusta and G. Rossi (1979) Fe/Mg distributions in the olivine of ultrafemic nodules from Assab (Ethiopia). *Neues Jahrb. Mineral. Monatsh.*, 197–202.

Birle, J. D., G. V. Gibbs, P. B. Moore and J. V. Smith (1968) Crystal structures of natural olivines. *Am. Mineral.*, 53, 807–824.

Brown, G. E. (1970) *Crystal Chemistry of the Olivines.* Ph.D. Thesis, Virginia Polytechnic Institute and State University, Blacksburg, Virginia.

——— and C. T. Prewitt (1973) High-temperature crystal chemistry of hortonolite. *Am. Mineral.*, 58, 577–587.

Burnham, C. W. (1973) Order–disorder relationships in some rock-forming minerals. *Annual Rev. Earth Planet. Sci.*, 1, 313–338.

Burns, R. G. (1970) *Mineralogical Applications of Crystal Field Theory.* Cambridge University Press, Cambridge, England.

Finger, L. W. (1970) Fe/Mg ordering in olivines. *Carnegie Inst. Wash. Year Book*, 69, 302–305.

——— and E. Prince (1975) A system of Fortran IV computer programs for crystal structure computations. *U.S. Natl. Bur. Stand. Tech. Note 854.*

——— and D. Virgo (1971) Confirmation of Fe/Mg ordering in olivines. *Carnegie Inst. Wash. Year Book*, 70, 221–225.

Francis, C. A. and P. H. Ribbe (1978) Crystal structures of the humite minerals: V. Magnesian manganhumite. *Am. Mineral.*, 63, 874–877.

Ganguli, D. (1977) Crystal chemical aspects of olivine structures. *Neues Jahrb. Mineral. Abh.*, 130, 303–318.

Ghose, S. (1962) The nature of $Mg^{2+}-Fe^{2+}$ distribution in some ferro-magnesian silicate minerals. *Am. Mineral.*, 47, 338–394.

——— and J. R. Weidner (1974) Site preference of transition metal ions in olivine (abstr.) *Geol. Soc. Am. Abstracts with Programs*, 6, 751.

———, C. Wan and I. S. McCallum (1976) $Fe^{2+} + Mg^{2+}$ order in an olivine from the lunar anorthosite 67075 and the significance of cation order in lunar and terrestrial olivines. *Indian J. Earth Sci.*, 3, 1–8.

———, ———, F. P. Okamura, H. Ohashi and J. R. Weidner (1976) Site preference and crystal chemistry of transition metal ions in pyroxenes and olivines. *Acta Crystallogr., A31 Supplement*, S76.

Hazen, R. M. (1976) Effects of temperature and pressure on the crystal structure of forsterite. *Am. Mineral.*, 61, 1280–1293.

International Tables for X-ray Crystallography, Vol. IV (1974) Kynoch Press, Birmingham, England.

Lager, G. A. and E. P. Meagher (1978) High-temperature structural study of six olivines. *Am. Mineral.*, 63, 365–377.

Rajamani, V., G. E. Brown and C. T. Prewitt (1975) Cation ordering in Ni–Mg olivine. *Am. Mineral.*, 60, 292–299.

Robinson, K., G. V. Gibbs and P. H. Ribbe (1971) Quadratic elongation: a quantitative measure of distortion in coordination polyhedra. *Science, 172*, 567–570.

Shannon, R. D. (1976) Revised effective ionic radii and systematic studies of interatomic distances in halides and chalcogenides. *Acta Crystallogr., A32*, 751–767.

Smyth, J. R. (1975) High temperature crystal chemistry of fayalite. *Am. Mineral.*, 60, 1092–1097.

——— and R. M. Hazen (1973) The crystal structures of forsterite and hortonolite at several temperatures up to 900°C. *Am. Mineral.*, 58, 588–593.

Walsh, D., G. Donnay and J. D. H. Donnay (1974) Jahn-Teller effect in ferro-magnesian minerals: pyroxene and olivines. *Bull. Soc. fr. Minéral. Cristallogr.*, 97, 170–183.

Wenk, H.-R. and K. N. Raymond (1973) Four new structure refinements of olivine. *Z. Kristallogr.*, 137, 86–105.